

## Spin Hall Effect with Space Inversion Symmetry

Nguyen Thanh Phuc<sup>1,2</sup> and Masahito Ueda<sup>3,4</sup><sup>1</sup>*Department of Theoretical and Computational Molecular Science,  
Institute for Molecular Science, 38 Nishigo-Naka, Myodaiji, Okazaki 444-8585, Japan*<sup>2</sup>*Department of Functional Molecular Science, SOKENDAI (The Graduate University for Advanced Studies),  
38 Nishigo-Naka, Myodaiji, Okazaki 444-8585, Japan*<sup>3</sup>*Department of Physics, University of Tokyo, 7-3-1 Hongo, Bunkyo-ku, Tokyo 113-0033, Japan*<sup>4</sup>*RIKEN Center for Emergent Matter Science (CEMS), Wako, Saitama 351-0198, Japan*

(Dated: February 22, 2019)

Unlike the conventional spin Hall effect (SHE) generated by the spin-orbit interaction which requires space-inversion-symmetry (SIS) breaking, we show that SHE can emerge in a broad class of many-body systems with SIS. Here the SHE arises from the dipole-dipole interaction (DDI) between particles which preserves SIS. As a concrete example, we show both analytically and numerically that the SHE can be observed in a system of ultracold heteronuclear molecules in an optical lattice. The DDI-induced SHE offers a complementary tool to generate spin currents, which constitutes an essential ingredient in spintronics.

PACS numbers: 03.75.Kk, 03.75.Mn, 67.85.Jk

*Introduction.* The spin Hall effect (SHE), first proposed for electrons by Dyakonov and Perel [1], is a phenomenon in which carriers feel a spin-dependent force that deflects their trajectories in a perpendicular direction. This force is similar to the Lorentz force in the Hall effect but has the opposite directions for spin-up and spin-down particles. With the SHE, one can generate a nonzero spin current  $\mathbf{j}_s = \mathbf{j}_\uparrow - \mathbf{j}_\downarrow$  at zero net particle current  $\mathbf{j} = \mathbf{j}_\uparrow + \mathbf{j}_\downarrow$  [2]. The SHE was first observed in GaAs [3–6] and later in a Bose-Einstein condensate (BEC) of <sup>87</sup>Rb subject to a spin-dependent artificial magnetic field [7] and in the propagation of light through the air-glass interface [8, 9]. Here, particles with (pseudo)spin-1/2 are electrons or atoms with hyperfine spin or photons, where the left- and right-circular polarizations play the role of two spin states. The SHE has found important applications in the field of spintronics as it is considered to be a practical tool for a new generation of magnetic random access memories [10, 11]. Moreover, the SHE also serves as an efficient mechanism to manipulate spins in antiferromagnets, which have inherent advantages over ferromagnets [12–14].

All of the SHEs observed to date were generated by the spin-orbit interaction (SOI), which emerges as a relativistic effect [15–17]. The SOI induces the SHE through either an intrinsic mechanism, in which particles experience a spin-dependent magnetic field generated directly by the SOI, or an extrinsic mechanism that requires an interplay between the SOI and impurity scattering in solid materials. Unlike the Hall effect, the SOI and SHE preserve time-reversal symmetry, and thus the SOI must be odd in momentum. As a result, the SOI only survives in systems where space inversion symmetry (SIS) is broken as in noncentrosymmetric zinc-blende or wurtzite semiconductors [17, 18] and quantum wells with broken structural inversion symmetry along the growth direc-

tion [19, 20]. In this Letter, we show that the SHE can emerge in systems with SIS. In particular, we demonstrate that the SHE can be realized in a diverse group of many-body systems whose particles possess electric or magnetic dipole moments. The particles interact with each other by the dipole-dipole interaction (DDI), which preserves SIS. Examples range from ultracold heteronuclear molecules (<sup>40</sup>K<sup>87</sup>Rb [21], <sup>87</sup>Rb<sup>133</sup>Cs [22, 23], <sup>23</sup>Na<sup>40</sup>K [24], <sup>23</sup>Na<sup>87</sup>Rb [25]), ultracold atoms with large magnetic dipole moments (<sup>52</sup>Cr [26], <sup>168</sup>Er [27], <sup>164</sup>Dy [28]), and Rydberg gases [29] to solid-state electronic materials with small or vanishing SOI, spin-triplet dimer excitations in quantum antiferromagnets [30], and nuclear spins of nitrogen-vacancy (NV) centers in diamond [31, 32]. As a concrete example, we investigate the spin dynamics of an ensemble of heteronuclear molecules loaded into an optical lattice [33] and show that the SHE can be observed in a typical time scale of experiments.

*SHE with SIS.* We first point out that the SHE can be realized without SIS breaking. Indeed, under space inversion, both the spin current density  $\mathbf{j}_s$  and the applied electric field  $\mathbf{E}$  change their signs, but the spin conductivity matrix  $\sigma_s$  remains unchanged ( $\mathbf{j}_s = \sigma_s \mathbf{E}$ ). The SHE is, therefore, compatible with the SIS and should appear in systems where the spin and orbital degrees of freedom (DOF) are coupled to each other in a way that preserves the SIS. To this end, the interaction Hamiltonian must be even in each of these DOF, which requires at least a two-body interaction  $H(\hat{\mathbf{s}}_i, \mathbf{s}_j, \mathbf{r}_{ij})$  unlike the SOI. Moreover, for the SHE we need an anisotropic interaction such that the spin DOF is coupled to a vectorial orbital DOF rather than a scalar one. The dipole-dipole interaction (DDI) [35]

$$H_{\text{dd}}(\hat{\mathbf{d}}_i, \hat{\mathbf{d}}_j, \mathbf{r}_{ij}) = C \frac{\hat{\mathbf{d}}_i \cdot \hat{\mathbf{d}}_j - 3(\hat{\mathbf{d}}_i \cdot \mathbf{e}_{ij})(\hat{\mathbf{d}}_j \cdot \mathbf{e}_{ij})}{4\pi r_{ij}^3}. \quad (1)$$

satisfies this requirement. Here  $r_{ij} = |\mathbf{r}_{ij}|$  is the distance between two dipole moments  $\hat{\mathbf{d}}_i$  and  $\hat{\mathbf{d}}_j$ ,  $\mathbf{e}_{ij} = \mathbf{r}_{ij}/r_{ij}$ , and  $C = 1/\epsilon_0$  ( $C = \mu_0$ ) for electric (magnetic) dipoles with  $\epsilon_0$  and  $\mu_0$  being the vacuum permittivity and the vacuum permeability, respectively. It is evident from Eq. (1) that the DDI preserves SIS as it is an even function of spatial coordinates. On the other hand, the DDI couples the spin and orbital degrees of freedom by conserving the total angular momentum, i.e., the sum of spin and orbital angular momenta. To make the spin-orbit coupling explicit, we decompose the DDI as  $H_{\text{dd}}(\hat{\mathbf{d}}_i, \hat{\mathbf{d}}_j, \mathbf{r}_{ij}) = H_{ij}^{\delta L=0} + H_{ij}^{\delta L=\pm 2}$  [36–38], where

$$H_{ij}^{\delta L=0} = \frac{C}{4\pi r_{ij}^3} \left( \frac{\hat{d}_i^{-1} \hat{d}_j^1 + \hat{d}_i^1 \hat{d}_j^{-1}}{2} + \hat{d}_i^z \hat{d}_j^z \right), \quad (2)$$

$$H_{ij}^{\delta L=\pm 2} = -\frac{3C}{8\pi r_{ij}^3} \left( \hat{d}_i^1 \hat{d}_j^1 e^{-2i\phi_{ij}} + \hat{d}_i^{-1} \hat{d}_j^{-1} e^{2i\phi_{ij}} \right). \quad (3)$$

Here,  $\hat{d}_j^{\pm 1} \equiv \mp(\hat{d}_j^x \pm i\hat{d}_j^y)/\sqrt{2}$  are the spherical harmonic components of the dipole-moment operator  $\hat{\mathbf{d}}_j$ , and  $(r_{ij}, \phi_{ij})$  are the polar coordinates of  $\mathbf{r}_{ij}$ . While  $H_{ij}^{\delta L=0}$  conserves both the spin and orbital angular momenta,  $H_{ij}^{\delta L=\pm 2}$  raises (lowers) the spin angular momentum by two and simultaneously lowers (raises) the orbital angular momentum by the same amount so as to conserve the total angular momentum. It is this spin-orbit coupling that gives rise to the DDI-based SHE proposed in this paper.

*SHE in molecular systems.* In the following, for the sake of concreteness we consider an example of a system of  $^{40}\text{K}^{87}\text{Rb}$  molecules loaded into a two-dimensional (2D) optical lattice in the  $xy$  plane [33] (see Fig. 1). They are subject to an external electric field  $\mathbf{E}$  that sets the quantization axis  $z$  of the internal (rotational) space. As shown below, the DDI-based SHE is clearly demonstrated in the Mott-insulator regime where the molecules are strongly localized at the lattice sites, leaving only the dynamics of their internal degrees of freedom. This regime can be realized by using a deep optical lattice potential [34]. Since the molecules are charge neutral and localized in coordinate space, the effect of  $\mathbf{E}$  on their external motion is irrelevant, and thus the SIS of the system is preserved. The rotational eigenstates  $|l, m_l\rangle$  of each molecule are indexed by the rotational and magnetic quantum numbers. The  $l = 1$  state manifold is separated from the  $|0, 0\rangle$  ground state by a rotational energy of  $2\epsilon_r$  where  $\epsilon_r = \hbar^2/(2I)$  with  $I$  being the moment of inertia of a molecule. Moreover, the applied electric field causes energy shifts of  $\delta\epsilon_{|1,0\rangle} \simeq \delta\epsilon \equiv (dE)^2/(6\epsilon_r)$  and  $\delta\epsilon_{|0,0\rangle} \simeq -\delta\epsilon$  for the two states ( $l = 0, 1$ ) with  $m_l = 0$ , where  $d$  is the permanent electric dipole moment of a molecule [39]. These energy shifts lift the degeneracy in the manifold of  $l = 1$  states. Since  $\delta\epsilon$  is typically much larger than the energy scale of the DDI, the system's dynamics governed by the DDI should essentially involve

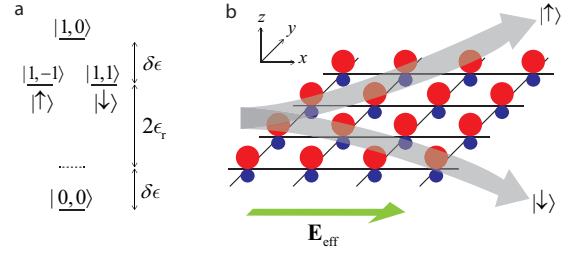


FIG. 1: Spin Hall effect (SHE) in a system of heteronuclear molecules interacting with each other by the dipole-dipole interaction (DDI). (a) Rotational lowest-energy levels  $|l, m_l\rangle$  of molecules with rotational ( $l$ ) and magnetic ( $m_l$ ) quantum numbers. The  $l = 1$  state manifold is separated from the  $|0, 0\rangle$  ground state by an energy of  $2\epsilon_r$ , and an external electric field further shifts the energies of two states  $|1, 0\rangle$  and  $|0, 0\rangle$  by  $+\delta\epsilon$  and  $-\delta\epsilon$ , respectively (see text for details). (b) Schematic illustration of the SHE. Heteronuclear molecules composed of two different atomic species (indicated by red and blue spheres) are placed at lattice sites of a two-dimensional optical lattice in the  $xy$  plane and interact with each other by the DDI. Their internal dynamics is mapped into a system of moving spin-1/2 particles in which two rotational levels  $|1, \pm 1\rangle$  represent the spin-up and spin-down states. An effective electric field  $\mathbf{E}_{\text{eff}}$  (green arrow) drives those particles in the  $x$  direction, and spin-up and spin-down particles are deflected oppositely towards the  $+y$  and  $-y$  directions, respectively. This DDI-based SHE produces a nonzero spin current at zero net particle current, which can directly be measured by a Stern-Gerlach experiment.

the three lowest energy levels:  $|0, 0\rangle$ ,  $|1, 1\rangle$  and  $|1, -1\rangle$ . Moreover, due to such an energy-scale separation, it is obvious from the energy-conservation consideration that  $H_{ij}^{\delta L=0}$  [Eq. (2)] exchanges the states  $|1, \pm 1\rangle$  and  $|1, 0\rangle$  between two molecules  $i$  and  $j$ , while  $H_{ij}^{\delta L=\pm 2}$  [Eq. (3)] transfers the state  $|1, \pm 1\rangle$  from one molecule to another followed by a spin flip ( $|1, \pm 1\rangle \rightarrow |1, \mp 1\rangle$ ) [40].

If the fraction of molecules in the excited states  $|1, \pm 1\rangle$  is small, the last term ( $\hat{d}_i^z \hat{d}_j^z$ ) in Eq. (2) becomes negligibly small compared with the other terms in the DDI. The dynamics of the internal degrees of freedom of molecules can be mapped onto that of a system of spin-1/2 particles where the two rotational levels  $|1, 1\rangle$  and  $|1, -1\rangle$  correspond to the spin-up and spin-down states, respectively, while the ground state  $|0, 0\rangle$  represents the vacuum for those excitations. The second-quantized DDI Hamiltonian of the system then reads as [38]

$$H_{\text{dd}} = t_0 \sum_{\substack{i,j \neq i \\ \sigma = \uparrow \downarrow}} \frac{\hat{b}_{i\sigma}^\dagger \hat{b}_{j\sigma}}{r_{ij}^3} - t_2 \sum_{i,j \neq i} \frac{e^{-2i\phi_{ij}} \hat{b}_{i\uparrow}^\dagger \hat{b}_{j\downarrow} + e^{2i\phi_{ij}} \hat{b}_{i\downarrow}^\dagger \hat{b}_{j\uparrow}}{r_{ij}^3}, \quad (4)$$

where  $\hat{b}_{j\sigma}$  ( $\hat{b}_{j\sigma}^\dagger$ ) is the annihilation (creation) operator of a particle with spin  $\sigma = \uparrow, \downarrow$  at lattice site  $j$ . The first term on the right-hand side of Eq. (4) describes a spin-conserving tunneling, while the second term describes

tunneling accompanied by a spin flip. The tunneling amplitudes are given by  $t_0 = Cd^2/(24\pi)$  and  $t_2 = 3t_0$  [39]. Due to the translation invariance of the system, the Hamiltonian  $H_{\text{dd}}$  can be expressed in terms of operators in momentum space as  $H_{\text{dd}} = \sum_{\mathbf{k}} (\hat{b}_{\mathbf{k}\uparrow}^\dagger, \hat{b}_{\mathbf{k}\downarrow}^\dagger) H \begin{pmatrix} \hat{b}_{\mathbf{k}\uparrow} \\ \hat{b}_{\mathbf{k}\downarrow} \end{pmatrix}$ , where

$$H = \begin{pmatrix} t_0 f^{(0)}(\mathbf{k}) & -t_2 f^{(2)}(\mathbf{k}) \\ -t_2 f^{(2)*}(\mathbf{k}) & t_0 f^{(0)}(\mathbf{k}) \end{pmatrix}, \quad (5)$$

$\hat{b}_{\mathbf{k}\sigma} \equiv (1/N^2) \sum_j e^{-i\mathbf{k}\cdot\mathbf{r}_j} \hat{b}_{j\sigma}$  ( $N$  is the number of lattice sites in one direction), and two functions  $f^{(0)}(\mathbf{k})$  and  $f^{(2)}(\mathbf{k})$  are given by  $f^{(0)}(\mathbf{k}) = N^2 \sum_{\mathbf{r}_j \neq 0} e^{-i\mathbf{k}\cdot\mathbf{r}_j} / r_j^3$  and  $f^{(2)}(\mathbf{k}) = N^2 \sum_{\mathbf{r}_j \neq 0} e^{-i\mathbf{k}\cdot\mathbf{r}_j} e^{2i\phi_j} / r_j^3$ , respectively. The energy eigenvalues and eigenstates of  $H_{\text{dd}}$  are then obtained through the diagonalization of Eq. (5), giving

$$H = E(\mathbf{0}) (\hat{b}_{\mathbf{0}\uparrow}^\dagger \hat{b}_{\mathbf{0}\uparrow} + \hat{b}_{\mathbf{0}\downarrow}^\dagger \hat{b}_{\mathbf{0}\downarrow}) + \sum_{\substack{\mathbf{k} \neq \mathbf{0} \\ \xi = \pm}} E_\xi(\mathbf{k}) \hat{b}_{\mathbf{k}\xi}^\dagger \hat{b}_{\mathbf{k}\xi}, \quad (6)$$

where  $E(\mathbf{0}) = t_0 f^{(0)}(\mathbf{k} = \mathbf{0})$ ,  $E_\pm(\mathbf{k}) = t_0 f^{(0)}(\mathbf{k}) \mp t_2 |f^{(2)}(\mathbf{k})|$  and  $\hat{b}_{\mathbf{k}+} = (e^{i\theta_{\mathbf{k}}} \hat{b}_{\mathbf{k}\uparrow} + \hat{b}_{\mathbf{k}\downarrow}) / \sqrt{2}$ ,  $\hat{b}_{\mathbf{k}-} = (\hat{b}_{\mathbf{k}\uparrow} - e^{-i\theta_{\mathbf{k}}} \hat{b}_{\mathbf{k}\downarrow}) / \sqrt{2}$  with  $\theta_{\mathbf{k}}$  being the phase of  $f^{(2)}(\mathbf{k})$ . In the following, we will show that the SHE emerges if an external force is applied to these spin-1/2 particles.

*Spin Hall conductivity.* We first consider the limit of a weak external force so that the linear-response theory can be used to find the spin Hall conductivity which measures the strength of the SHE in the system. Since the spin-up and spin-down particles correspond to the  $|1, \pm 1\rangle$  excitations of the molecules, a force exerted on those particles can be generated by, for example, a spatial gradient of the applied electric field which makes a spatially dependent energy difference of  $2B_r + \delta\epsilon(\mathbf{r})$  between  $|1, \pm 1\rangle$  and  $|0, 0\rangle$  states. This force plays the role of an effective electric field for the spin-1/2 particles, which can be expressed in terms of an effective vector potential as  $\mathbf{E}_{\text{eff}}(\mathbf{r}, t) = \partial \mathbf{A}_{\text{eff}}(\mathbf{r}, t) / \partial t$ . In the presence of a vector potential, the Hamiltonian  $H$  of the system is obtained by replacing the momentum operator  $\hat{\mathbf{p}}$  by  $\hat{\mathbf{p}} - \mathbf{A}_{\text{eff}}(\hat{\mathbf{r}}, t)$  to ensure the local gauge invariance. The first-order perturbation of the Hamiltonian is given by  $\delta H = - \int d\mathbf{r} \hat{\mathbf{j}}^{\text{p}}(\mathbf{r}) \cdot \mathbf{A}_{\text{eff}}(\mathbf{r}, t)$ , where  $\hat{\mathbf{j}}^{\text{p}}(\mathbf{r}) = \frac{1}{2} \{ \hat{n}(\mathbf{r}), \hat{\mathbf{v}} \}$  is the paramagnetic component of the particle-current density operator [41]. Here, the curly brackets denote the anticommutator and the particle-density and group-velocity operators are given by  $\hat{n}(\mathbf{r}) = \delta(\mathbf{r} - \hat{\mathbf{r}})$  and  $\hat{\mathbf{v}} = \frac{\partial H}{\partial \hat{\mathbf{p}}}$ , respectively. From Eq. (5), the group-velocity

operator is found to be

$$\hat{\mathbf{v}} = \frac{1}{\hbar} \begin{pmatrix} t_0 \mathbf{g}^{(0)}(\hat{\mathbf{p}}/\hbar) & -t_2 \mathbf{g}^{(2)}(\hat{\mathbf{p}}/\hbar) \\ -t_2 \mathbf{g}^{(2)*}(\hat{\mathbf{p}}/\hbar) & t_0 \mathbf{g}^{(0)}(\hat{\mathbf{p}}/\hbar) \end{pmatrix}, \quad (7)$$

where  $\mathbf{g}^{(0),(2)}(\mathbf{k}) \equiv \nabla_{\mathbf{k}} f^{(0),(2)}(\mathbf{k})$ . The total particle-current density is the sum of the paramagnetic and diamagnetic components, where the latter is given by the product of the particle density and the vector potential. In the linear-response regime, the paramagnetic particle-current density in the frequency domain is given by  $j_\alpha^{\text{p}}(\mathbf{r}, \omega) = \sum_\beta \int d\mathbf{r}' K_{\alpha,\beta}(\mathbf{r}, \mathbf{r}', \omega) A_\beta(\mathbf{r}', \omega)$ , where  $\alpha, \beta = x, y, z$  and  $K_{\alpha,\beta}(\mathbf{r}, \mathbf{r}', \omega)$  is the paramagnetic response function. On the other hand, since the total particle current should vanish at the zero-frequency limit, where the vector potential becomes time independent, leading to the vanishing electric field, the diamagnetic current can be expressed in terms of the paramagnetic response function  $K_{\alpha,\beta}(\mathbf{r}, \mathbf{r}', \omega = 0)$  at zero frequency. Summing the two components, we obtain the total particle-current density as  $j_\alpha(\mathbf{r}, \omega) = \sum_\beta \int d\mathbf{r}' [K_{\alpha,\beta}(\mathbf{r}, \mathbf{r}', \omega) - K_{\alpha,\beta}(\mathbf{r}, \mathbf{r}', \omega = 0)] A_\beta(\mathbf{r}', \omega)$ . Now, the spin-current density operator with the  $z$ -axis polarization is given by  $\hat{\mathbf{j}}_s^z(\mathbf{r}) = \frac{\hbar}{4} \{ \hat{\sigma}_z, \hat{\mathbf{j}}(\mathbf{r}) \}$ , where  $\hat{\sigma}_z = \text{diag}(1, -1)$  is the Pauli matrix [6]. This spin current can be measured directly by the Stern-Gerlach experiment [42]. As the vector potential is related to the electric field in the frequency domain by  $\mathbf{A}(\mathbf{r}, \omega) = \mathbf{E}(\mathbf{r}, \omega) / (i\omega)$ , the spin conductivity matrix is given by

$$(\chi_s)_{\alpha\beta}(\mathbf{r}, \mathbf{r}', \omega) = \frac{(K_s)_{\alpha,\beta}(\mathbf{r}, \mathbf{r}', \omega) - (K_s)_{\alpha,\beta}(\mathbf{r}, \mathbf{r}', \omega = 0)}{i\omega}, \quad (8)$$

where  $(K_s)_{\alpha,\beta}(\mathbf{r}, \mathbf{r}', \omega)$  is the paramagnetic response function of the spin current.

To preserve the SIS, suppose that half of the spin-1/2 particles are initially prepared in the eigenstate  $|\Psi_1\rangle = |\mathbf{q}, +\rangle$  of the Hamiltonian (6) with a momentum  $\hbar\mathbf{q} \neq 0$  and the other half in the eigenstate  $|\Psi_2\rangle = |-\mathbf{q}, +\rangle$ . Such an initial state can be realized, for example, by using a pair of independent counter-propagating laser beams with appropriately chosen directions and polarizations to excite the molecular ensemble. Note that in contrast with the case of the Rashba SOI, here the spin components of  $|\mathbf{q}, +\rangle$  and  $|-\mathbf{q}, +\rangle$  are identical, reflecting the SIS which is conserved by the DDI. Using the linear-response theory [39], the paramagnetic response function is found to be

$$(K_s)_{\alpha\beta}(\mathbf{r}, \mathbf{r}', \omega) = -\frac{1}{4\pi} \sum_{j=1}^2 \sum_n \left[ \frac{\langle \Psi_j | (\hat{j}_s^P)_\alpha^z(\mathbf{r}) | \psi_n \rangle \langle \psi_n | \hat{j}_\beta^P(\mathbf{r}') | \Psi_j \rangle}{E_0 - E_n - \hbar\omega + i\eta} + \frac{\langle \psi_n | (\hat{j}_s^P)_\alpha^z(\mathbf{r}) | \Psi_j \rangle \langle \Psi_j | \hat{j}_\beta^P(\mathbf{r}') | \psi_n \rangle}{E_0 - E_n + \hbar\omega - i\eta} \right], \quad (9)$$

where  $\eta$  is an infinitesimal positive number and the sum is taken over all eigenstates  $|\psi_n\rangle$  of Hamiltonian (6). Here  $E_0$  is the eigenenergy of  $|\Psi_{1,2}\rangle$  and  $E_n$  is that of  $|\psi_n\rangle$ . The matrix elements in Eq. (9) can be evaluated straightforwardly [39]. As the unperturbed system is translation invariant, both  $(K_s)_{\alpha\beta}(\mathbf{r}, \mathbf{r}', \omega)$  and  $(\chi_s)_{\alpha\beta}(\mathbf{r}, \mathbf{r}', \omega)$  are

functions of  $\mathbf{r} - \mathbf{r}'$ . By making the Fourier transformation  $(\chi_s)_{\alpha\beta}(\mathbf{k}, \omega) = \int d(\mathbf{r} - \mathbf{r}') e^{-i\mathbf{k}\cdot(\mathbf{r} - \mathbf{r}')} (\chi_s)_{\alpha\beta}(\mathbf{r} - \mathbf{r}', \omega)$  and taking the limit of  $\mathbf{k} \rightarrow \mathbf{0}$  and  $\omega \rightarrow 0$ , which corresponds to a homogeneous and static driving force, we obtain

$$(\chi_s)_{\alpha\beta}(\mathbf{k} \rightarrow \mathbf{0}, \omega \rightarrow 0) = -\frac{t_0 t_2}{2\pi S} \sum_{\mathbf{p}=\pm\mathbf{q}} \frac{g_\alpha^{(0)}(\mathbf{p}) \text{Im} \left\{ e^{i\theta_{\mathbf{p}}} \left[ -g_\beta^{(2)}(\mathbf{p} + e^{2i\theta_{\mathbf{p}}} g_\beta^{(2)}(\mathbf{p})^* \right] \right\}}{[E_+(\mathbf{p}) - E_-(\mathbf{p})]^2}, \quad (10)$$

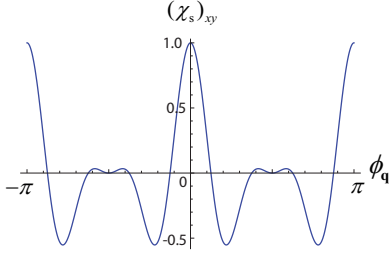


FIG. 2: Dependence of the spin Hall conductivity  $(\chi_s)_{xy}$  on the direction of the initial excitation with wavevector  $\mathbf{q}$ . Here  $\mathbf{q} = (q, \phi_{\mathbf{q}})$  are the polar coordinates, and  $(\chi_s)_{xy}$  is shown in units of  $1/[\pi(Nqa)^2]$ , where  $a$  and  $N$  are the lattice constant and the number of lattice sites in one dimension, respectively.

where  $S = (Na)^2$  is the area of the lattice. In the long-wavelength limit  $ka \ll 1$  ( $a$  is the lattice constant) and for the square lattice,  $f^{(0)}(\mathbf{k})$  and  $f^{(2)}(\mathbf{k})$  have the asymptotic forms of  $a^3 f^{(0)}(\mathbf{k})/N^2 \simeq A - 2\pi ka$  and  $a^3 f^{(2)}(\mathbf{k})/N^2 \simeq 2\pi i k a e^{2i\phi_{\mathbf{k}}}/3$ , respectively, where  $A \simeq 9.03$  is a constant and  $\phi_{\mathbf{k}}$  is the azimuthal angle of  $\mathbf{k}$  [39]. Therefore, for  $qa \ll 1$  the spin Hall conductivity  $(\chi_s)_{xy}(\mathbf{k} \rightarrow \mathbf{0}, \omega \rightarrow 0)$  reduces to

$$(\chi_s)_{xy} = \frac{\cos(4\phi_{\mathbf{q}}) \cos^2(\phi_{\mathbf{q}})}{\pi(Nqa)^2}. \quad (11)$$

The dependence of  $(\chi_s)_{xy}$  on the direction of the initial excitation, i.e., on the angle  $\phi_{\mathbf{q}}$ , is shown in Fig. 2, showing the anisotropic nature of the DDI [Eq. (1)] with the  $\pi$ -periodicity, reflecting the SIS preserved by the DDI.

*Numerical simulation.* As mentioned above Eq. (4), in deriving analytically the spin Hall conductivity [Eq. (11)], we have assumed that the fraction of molecu-

lar excitations, i.e., the ratio of the number of molecules in the  $|1, \pm 1\rangle$  rotational state to that of molecules in the  $|0, 0\rangle$  state, is sufficiently small so that the interaction between excitations [the last term in Eq. (2)] can be neglected. As numerically demonstrated below, this assumption can be removed without changing qualitatively the physics we are interested in.

In the numerical simulation, molecules are located at the sites of a  $3 \times 3$  square lattice with unit filling, i.e., one molecule per site. Initially, all molecules are prepared in the  $|0, 0\rangle$  rotational ground state. Molecules in the left edge are then excited to the superposition state:  $(|1, 1\rangle + |1, -1\rangle)/\sqrt{2}$  (see Fig. 3a). An effective electric field  $\mathbf{E}_{\text{eff}}$  for those excitations is applied in the  $x$  direction as described by an energy potential  $H_E = E_{\text{eff}} \sum_j x_j \hat{P}_j^0$ , where  $x_j$  and  $\hat{P}_j^0$  are the  $x$ -coordinate and projection operator onto the  $|0, 0\rangle$  ground state of the molecule at lattice site  $j$ , respectively. The time evolution of the system is obtained by using the exact diagonalization method [39].

Figure 3b shows the short-time dynamics of the  $z$ -polarization  $M_z(x_j, y_j) = \langle \hat{P}_j^1 - \hat{P}_j^{-1} \rangle$  of molecules at four lattice sites  $(x_j, y_j) = (1, 2), (1, 3), (3, 2)$  and  $(3, 3)$ . Here,  $\hat{P}_j^{\pm 1}$  are the projection operators onto the rotational states  $|1, \pm 1\rangle$  of a molecule at lattice site  $j$ . It is evident that  $M_z$  negatively increases for molecules at the bottom edge and positively increases for molecules at the top edge, while their absolute values are almost equal. This implies the existence of flows of particles in the  $\pm y$  directions with equal strengths but opposite spins, i.e., the SHE. The time scale of the spin Hall dynamics shown in Fig. 3b is given by  $\tau = \hbar/\epsilon_{\text{dd}}$ , where  $\epsilon_{\text{dd}} = Cd^2/(4\pi a^3)$  is the characteristic energy scale of the DDI. Using the

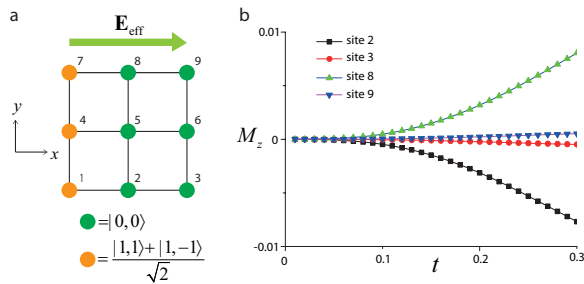


FIG. 3: Dynamical simulation of the spin Hall effect in a molecular system with the dipole-dipole interaction (DDI). (a) Initially, all molecules are prepared in the  $|0, 0\rangle$  rotational ground state (green circles). Molecules at the left edge are excited to the superposition state:  $(|1, 1\rangle + |1, -1\rangle)/\sqrt{2}$  (orange circles). An effective electric field  $\mathbf{E}_{\text{eff}}$  is applied in the  $x$  direction, whose magnitude is taken to be  $E_{\text{eff}}a = \epsilon_{\text{dd}}/4$ , where  $\epsilon_{\text{dd}} = Cd^2/(4\pi a^3)$  is the characteristic energy scale of the DDI. (b) Time evolutions of the  $z$ -polarization  $M_z(\mathbf{r}_j) = \langle \hat{P}_j^1 - \hat{P}_j^{-1} \rangle$  of molecules at four lattice sites. Here,  $\hat{P}_j^{\pm 1}$  are the projection operators onto the rotational states  $|1, \pm 1\rangle$  at lattice site  $j$ . The time  $t$  is measured in units of  $\hbar/\epsilon_{\text{dd}}$ .

parameters of the  $^{40}\text{K}^{87}\text{Rb}$  molecule [21], we find that  $\tau \simeq 0.5$  ms, which makes the DDI-based SHE observable in current experiments.

*Conclusion.* We have proposed the spin Hall effect (SHE) without space inversion symmetry (SIS) breaking, unlike the ordinary SHE which is generated by the spin-orbit interaction (SOI). To give support for this argument, we have shown both analytically and numerically that the SHE can emerge in systems whose particles undergo the dipole-dipole interaction (DDI), which preserves SIS. As a concrete example, we have investigated the SHE in a system of heteronuclear molecules such as  $^{40}\text{K}^{87}\text{Rb}$ ; however, the SHE can, in principle, be observed in a wide range of systems including ultracold magnetic atoms [26–28, 43], Rydberg excitations [29], electron gases, quantum antiferromagnets [30], and NV centers [31, 32].

It should be emphasized that here the SIS is preserved both in the Hamiltonian through the DDI and in the system’s dynamics as reflected by a nonzero spin Hall conductivity for a space-inversion-symmetric initial state. This is in marked contrast with the case of parity-breaking phases in spin-orbit-coupled metals with SIS where a spontaneous symmetry breaking of the SIS occurs due to Fermi liquid instabilities [44]. It is also noteworthy that in contrast with ultracold atoms and molecules treated in this work, which are perfectly clean systems with no defects, the effect of impurity scattering becomes relevant in evaluating the spin Hall effect in solid-state electronic systems. In particular, it is necessary to take account of the vertex correction, which can dramatically change the spin Hall conductivity as shown in the case of an electron gas with the Rashba SOI [45].

Concerning the strength of interaction, although the magnitude of magnetic DDI is generally smaller than that of the electric DDI by a factor of  $\alpha^2$ , where  $\alpha = e^2/(4\pi\epsilon_0\hbar c)$  is the fine structure constant, the magnetic DDI and the electric SOI have the same scaling with respect to the fine structure constant. Therefore, the DDI-based SHE proposed in this paper can find its importance in not only systems whose particles possess a huge electric dipole moment but also in numerous space-inversion-symmetric systems with magnetic dipole moments where the SOI is negligible.

Unlike the SHE based on SOI, which is a one-body effect, the DDI-based SHE is a genuine many-body phenomenon. Furthermore, using the SOI, the quantum SHE characterized by a unidirectional edge spin transport, i.e., edge states with opposite spins propagating in opposite directions, has been observed in both electronic [46, 47] and photonic [48] materials, and it gives rise to a new and important class of materials, namely topological insulators [49, 50]. Similarly, the DDI-based SHE can open a research avenue towards engineering as yet unexplored classes of many-body topological materials in which the inter-particle interaction plays a vital role.

This work was supported by KAKENHI Grant No. 26287088 from the Japan Society for the Promotion of Science, and a Grant-in-Aid for Scientific Research on Innovation Areas “Topological Quantum Phenomena” (KAKENHI Grant No. 22103005), and the Photon Frontier Network Program from MEXT of Japan.

- 
- [1] M. I. Dyakonov, V. I. Perel, Possibility of orienting electron spins with current. *Sov. Phys. JETP* **13**, 467–469 (1971).
  - [2] J. Sinova, S. O. Valenzuela, J. Wunderlich, C. H. Back, T. Jungwirth, Spin Hall effects. *Rev. Mod. Phys.* **87**, 1213 (2015).
  - [3] Y. K. Kato, R. C. Myers, A. C. Gossard, D. D. Awschalom, Observation of the spin Hall effect in semiconductors. *Science* **306**, 1910–1913 (2004).
  - [4] J. Wunderlich, B. Kaestner, J. Sinova, T. Jungwirth, Experimental observation of the spin-Hall effect in a two-dimensional spin-orbit coupled semiconductor system. *Phys. Rev. Lett.* **94**, 047204 (2005).
  - [5] S. Murakami, N. Nagaosa, S. C. Zhang, Dissipationless quantum spin current at room temperature. *Science* **301**, 1348 (2003).
  - [6] J. Sinova, D. Culcer, Q. Niu, N. A. Sinitsyn, T. Jungwirth, A. H. MacDonald, Universal Intrinsic Spin Hall Effect. *Phys. Rev. Lett.* **92**, 126603 (2004).
  - [7] M. C. Beeler, R. A. Williams, K. Jimenez-Garcia, L. J. LeBlanc, A. R. Perry, I. B. Spielman, The spin Hall effect in a quantum gas. *Nature* **498**, 201 (2013).
  - [8] O. Hosten, P. Kwiat, Observation of the spin Hall effect of light via weak measurements. *Science* **319**, 787–790 (2008).

- [9] M. Onoda, S. Murakami, N. Nagaosa, Hall Effect of Light. *Phys. Rev. Lett.* **93**, 083901 (2004).
- [10] J. Sinova, T. Jungwirth, Surprises from the spin Hall effect. *Physics Today* **70**, 7, 38 (2017).
- [11] J. Sinova, I. Zutic, New moves of the spintronics tango. *Nat. Mater.* **11**, 368 (2012).
- [12] J. Zelezny, H. Gao, K. Vyborny, J. Zemen, J. Masek, A. Manchon, A. Wunderlich, J. Sinova, T. Jungwirth, Relativistic Neel-Order Fields Induced by Electrical Current in Antiferromagnets *Phys. Rev. Lett.* **113**, 157201 (2014).
- [13] P. Wadley, B. Howells, J. Zelezny, C. Andrews, V. Hills, R. P. Campion, V. Novak, K. Olejnik, F. Maccherozzi, S. S. Dhesi, S. Y. Martin, T. Wagner, J. Wunderlich, F. Freimuth, Y. Mokrousov, J. Kunes, J. S. Chauhan, M. J. Grzybowski, A. W. Rushforth, K. W. Edmonds, B. L. Gallagher, T. Jungwirth, Electrical switching of an antiferromagnet. *Science* **351**, 587 (2016).
- [14] K. Olejnik, V. Schuler, X. Marti, V. Novak, Z. Kaspar, P. Wadley, R. P. Campion, K. W. Edmonds, B. L. Gallagher, J. Garces, M. Baumgartner, P. Gambardella, T. Jungwirth, Antiferromagnetic CuMnAs multi-level memory cell with microelectronic compatibility. *Nat. Comm.* **8**, 15434 (2017).
- [15] A. Manchon, H. C. Koo, J. Nitta, S. M. Frolov, R. A. Duine, New perspectives for Rashba spinorbit coupling, *Nat. Mat.* **14**, 871 (2015).
- [16] E. Rashba, Properties of semiconductors with an extremum loop. 1. Cyclotron and combinational resonance in a magnetic field perpendicular to the plane of the loop. *Sov. Phys. Solid State* **2**, 1109–1122 (1960).
- [17] G. Dresselhaus, Spin-orbit coupling effects in zinc blende structures, *Phys. Rev.* **100**, 580–586 (1955).
- [18] M. I. Dyakonov, V. Y. Kachorovskii, Spin relaxation of two-dimensional electrons in noncentrosymmetric semiconductors. *Sov. Phys. Semicond.* **20**, 110112 (1986).
- [19] F. T. Vasko, Spin splitting in the spectrum of two-dimensional electrons due to the surface potential. *P. Zh. Eksp. Teor. Fiz.* **30**, 574577 (1979).
- [20] Y. A. Bychkov, E. I. Rashba, Properties of a 2D electron gas with lifted spectral degeneracy. *P. Zh. Eksp. Teor. Fiz.* **39**, 6669 (1984).
- [21] K.-K. Ni, S. Ospelkaus, M. H. G. de Miranda, A. Pefer, B. Neyenhuis, J. J. Zirbel, S. Kotochigova, P. S. Julienne, D. S. Jin, J. Ye, A High Phase-Space-Density Gas of Polar Molecules, *Science* **322**, 231 (2008).
- [22] T. Takekoshi, L. Reichsollner, A. Schindewolf, J. M. Hutson, C. R. L. Sueur, O. Dulieu, F. Ferlaino, R. Grimm, H.-C. Nagerl, Ultracold dense samples of dipolar RbCs molecules in the rovibrational and hyperfine ground state. *Phys. Rev. Lett.* **113**, 205301 (2014).
- [23] P. K. Molony, P. D. Gregory, Z. Ji, B. Lu, M. P. Koppinger, C. R. L. Sueur, C. L. Blackley, J. M. Hutson, S. L. Cornish, Creation of ultracold  $^{87}\text{Rb}^{133}\text{Cs}$  molecules in the rovibrational ground state. *Phys. Rev. Lett.* **113**, 255301 (2014).
- [24] J. W. Park, S. A. Will, M. W. Zwierlein, Ultracold dipolar gas of fermionic  $^{23}\text{Na}^{40}\text{K}$  molecules in their absolute ground state. *Phys. Rev. Lett.* **114**, 205302 (2015).
- [25] M. Guo, B. Zhu, B. Lu, X. Ye, F. Wang, R. Vexiau, N. Bouloufa-Maafa, G. Quemener, O. Dulieu, D. Wang, Creation of an ultracold gas of ground-state dipolar  $^{23}\text{Na}^{87}\text{Rb}$  molecules. *Phys. Rev. Lett.* **116**, 205303 (2016).
- [26] A. Griesmaier, J. Werner, S. Hensler, J. Stuhler, T. Pfau, Bose-Einstein Condensation of Chromium, *Phys. Rev. Lett.* **94**, 160401 (2005).
- [27] K. Aikawa, A. Frisch, M. Mark, S. Baier, A. Rietzler, R. Grimm, F. Ferlaino, Bose-Einstein Condensation of Erbium, *Phys. Rev. Lett.* **108**, 210401 (2012).
- [28] M. Lu, N. Q. Burdick, S. H. Youn, B. L. Lev, Strongly Dipolar Bose-Einstein Condensate of Dysprosium, *Phys. Rev. Lett.* **107**, 190401 (2011).
- [29] M. Kiffner, W. Li, D. Jaksch, Three-Body Bound States in Dipole-Dipole Interacting Rydberg Atoms, *Phys. Rev. Lett.* **111**, 233003 (2013).
- [30] S. Auerbach, *Interacting Electrons and Quantum Magnetism* (Springer, New York, 1994).
- [31] F. Jelezko, T. Gaebel, I. Popa, M. Domhan, A. Gruber, J. Wrachtrup, Observation of Coherent Oscillation of a Single Nuclear Spin and Realization of a Two-Qubit Conditional Quantum Gate, *Phys. Rev. Lett.* **93**, 130501 (2004).
- [32] G. Kucsko, S. Choi, J. Choi, P. C. Maurer, H. Sumiya, S. Onoda, J. Isoya, F. Jelezko, E. Demler, N. Y. Yao, M. D. Lukin, Critical thermalization of a disordered dipolar spin system in diamond, arXiv:1609.08216 (2016).
- [33] S. A. Moses, J. P. Covey, M. T. Miecnikowski, B. Yan, B. Gadway, J. Ye, D. S. Jin, Creation of a low-entropy quantum gas of polar molecules in an optical lattice, *Science* **350**, 659 (2015).
- [34] B. Yan, S. A. Moses, B. Gadway, J. P. Covey, K. R. A. Hazzard, A. M. Rey, D. S. Jin, J. Ye, Observation of dipolar spin-exchange interactions with lattice-confined polar molecules, *Nature* **501**, 521 (2013).
- [35] J. D. Jackson, *Classical Electrodynamics* (John Wiley & Sons, ed. 3, 1999).
- [36] P. Pasquiou, G. Bismut, Q. Beaufils, A. Crubellier, E. MarLechal, P. Pedri, L. Vernac, O. Gorceix, B. Laburthe-Tolra, Control of dipolar relaxation in external fields, *Phys. Rev. A* **81**, 042716 (2010).
- [37] A. de Paz, A. Chotia, E. MarLechal, P. Pedri, L. Vernac, O. Gorceix, B. Laburthe-Tolra, Resonant demagnetization of a dipolar Bose-Einstein condensate in a three-dimensional optical lattice, *Phys. Rev. A* **87**, 051609 (2013).
- [38] S. V. Syzranov, M. L. Wall, V. Gurarie, A. M. Rey, Spin-orbital dynamics in a system of polar molecules, *Nat. Comm.* **5**, 5391 (2014).
- [39] See Supplemental Material for additional information on the molecular energy levels in the presence of an external electric field, the mapping of the DDI between molecules to a long-range tunneling of spin-1/2 particles, the linear response theory, the evaluation of matrix elements in the linear response function, the asymptotic forms of functions  $f^{(0)}(\mathbf{k})$  and  $f^{(2)}(\mathbf{k})$ , and the exact diagonalization.
- [40] The term  $\hat{d}_i^1 \hat{d}_j^1$  in Eq. (3) causes the state transition at site  $i$  ( $j$ ) from  $|1, -1\rangle$  ( $|0, 0\rangle$ ) to  $|0, 0\rangle$  ( $|1, 1\rangle$ ), which implies that the state  $|1, -1\rangle$  is transferred from  $i$  to  $j$  followed by a spin flip  $|1, -1\rangle \rightarrow |1, 1\rangle$ . Similarly, the term  $\hat{d}_i^{-1} \hat{d}_j^{-1}$  causes the state transition at site  $i$  ( $j$ ) from  $|1, 1\rangle$  ( $|0, 0\rangle$ ) to  $|0, 0\rangle$  ( $|1, -1\rangle$ ), which implies that the state  $|1, 1\rangle$  is transferred from  $i$  to  $j$  followed by a spin flip  $|1, 1\rangle \rightarrow |1, -1\rangle$ .
- [41] J. Rammer, *Quantum Transport Theory* (Perseus Books, 1998).
- [42] W. Gerlach, O. Stern, Der experimentelle Nachweis der Richtungsquantelung im Magnetfeld. *Zeitschrift für*

- Physik **9**, 349352 (1922).
- [43] T. Oshima, Y. Kawaguchi, Spin Hall effect in a spinor dipolar Bose-Einstein condensate. *Phys. Rev. A* **93**, 053605 (2016).
- [44] L. Fu, Parity-Breaking Phases of Spin-Orbit-Coupled Metals with Gyrotropic, Ferroelectric, and Multipolar Orders, *Phys. Rev. Lett.* **115**, 026401 (2015).
- [45] J. Inoue, G. E. Bauer, and L. W. Molenkamp, Suppression of the persistent spin Hall current by defect scattering, *Phys. Rev. B* **70**, 041303 (2004).
- [46] C. L. Kane, E. J. Mele,  $Z_2$  Topological Order and the Quantum Spin Hall Effect. *Phys. Rev. Lett.* **95**, 146802 (2005).
- [47] B. A. Bernevig, T. L. Hughes, S. C. Zhang, Quantum spin Hall effect and topological phase transition in HgTe quantum wells. *Science* **314**, 1757–1761 (2006).
- [48] K. Y. Bliokh, D. Smirnova, F. Nori, Quantum spin Hall effect of light. *Science* **348**, 1448 (2015).
- [49] M. Z. Hasan, C. L. Kane, Colloquium: Topological insulators. *Rev. Mod. Phys.* **82**, 3045–3067 (2010).
- [50] X.-L. Qi, S.-C. Zhang, Topological insulators and superconductors. *Rev. Mod. Phys.* **83**, 1057–1110 (2011).